Available online at www.sciencedirect.com
ScienceDirect
Marine Chemistry 103 (2007) 15–29
MARINE CHEMISTRY
www.elsevier.com/locate/marchem

An integrated geochemical and hydrodynamic model for tidal coastal environments

Jian Peng [a,*], Eddy Y. Zeng [b]

[a] Southern California Coastal Water Research Project, 7171 Fenwick Lane, Westminster, CA 92683, USA
[b] State Key Laboratory of Organic Geochemistry, Guangzhou Institute of Geochemistry, Chinese Academy of Sciences, Guangzhou 510640, China

Received 24 May 2006; accepted 31 May 2006
Available online 12 July 2006

Abstract

In this paper, the design, calibration and application of an integrated geochemical–hydrodynamic model are described. The model comprises three parts: A hydrodynamic submodel that was adopted from a depth-averaged, semi-implicit hydrodynamic model, a geochemical submodel based on equilibrium partitioning of chemicals between aqueous and particulate phases, and a particle dynamic submodel that simulates resuspension, transport and settling of suspended particulate matter (SPM). The integrated model was implemented in San Diego Bay (SDB), a heavily urbanized, semi-closed mesotidal embayment. A series of model calibrations were carried out based on observations on salinity, polychlorinated biphenyls (PCBs) and SPM. Salinity calibrations indicated that only 15% of precipitation in the drainage area of SDB could reach the bay, presumably due to the dams on the tributary rivers. Steady-state calibrations of PCBs based on fixed concentrations at known 'hot spots' have reproduced observed PCB concentrations in both the dissolved and particulate phases. SPM calibrations showed that shipping-induced resuspension produce more SPM than natural processes. Based on the calibrated model, the annual transport of PCBs out of SDB was estimated to be 3.85 kg (3.5 kg and 0.35 kg in the dissolved and particulate phases, respectively), much higher than the previous estimates based on steady-state assumptions. It was also found out that only a small portion of the fine sediment exported from SDB was derived from riverine input. This model can be applied to the studies of the transport and fate of other chemical species. It can be transplanted to other coastal areas as well. The integrated model represents a novel framework in which geochemical processes in coastal environments can be investigated on a truly dynamic basis.

Keywords: Geochemical; Hydrodynamic; Modeling; San Diego Bay; PCB; SPM

1. Introduction

In shallow coastal seas, many biogeochemical processes are controlled directly or indirectly by hydrodynamics. These processes include diffusion, dispersion, and transport of solutes, sediment–water interaction, and adsorption–desorption of chemicals to and from suspended particulate matter (SPM). Processes within the sediment column, though of much longer time scales, can be affected indirectly by hydrodynamics in the overlying water column through sediment–water interactions. If water column hydrodynamics is quantitatively defined, these related processes may be studied dynamically and quantitatively in both the temporal and spatial domains.

* Corresponding author. Tel.: +1 714 372 9223; fax: +1 714 894 9699.
E-mail address: jianp@sccwrp.org (J. Peng).

0304-4203/$ - see front matter © 2006 Elsevier B.V. All rights reserved.
doi:10.1016/j.marchem.2006.05.007

For example, in a study area where hydrodynamic parameters such as velocity, turbulence, water surface elevation and density are defined in each time step at every computational grid, it is possible to quantitatively study the behavior and environmental fate of chemical species of concern by defining processes such as diffusion and advection, adsorption and desorption, chemical and biological transformation, among others (Christiansen et al., 2000; James, 2002; Karickhoff et al., 1979; Lumborg and Windelin, 2003; Martin and McCutcheon, 1999; McDonald and Cheng, 1994).

Recent advances in the numerical modeling techniques have enabled simulations of physical processes of coastal oceans in great detail and with high accuracy, allowing forecasting and nowcasting of oceanic conditions such as tides, currents and waves (Cheng et al., 1993; Wang et al., 1998). However, the applications of these hydrodynamic models on the transport and fate of environmentally significant chemical species remain limited, especially for those chemicals that are associated with particulate matter. The difficulties originate from the fact that particle dynamic modeling itself is a nontrivial task. Equations describing particle resuspension and settling (two key processes in particle dynamics) are still largely empirical and rigid.

Applying these equations to a new study area requires a considerable amount of measurements and calibrations to select the optimal values for a large number of empirical constants (Christiansen et al., 2000; McDonald and Cheng, 1994; Taki, 2001). Consequently, the difficulty propagates to the modeling of particle-reactive chemical species, in which a reliable simulation of particle dynamics is a prerequisite.

Moreover, the difficulty of establishing an integrated geochemical and hydrodynamic model lies in the demanding task of calibration and verification of the geochemical model. In order to calibrate a geochemical model, one will need a large number of chemical analyses with sufficient temporal and spatial coverage as well as frequency. For chemical species of very low concentrations such as many trace organic contaminants, time-series measurements are often costly or simply impossible. As a result, as long as the hydrodynamic model is properly calibrated and verified, a compromise is often needed in terms of calibration and verification of chemical model. For example, the sampling for ppb-level chemicals may not necessarily represent a 'snapshot' because the sampling time can be as long as a few days.

To address the above issues and establish a novel approach to studying transport and geochemical processes of non-conservative chemicals in coastal oceans, an integrated geochemical and hydrodynamic model is needed. To this end, an existing depth-averaged hydrodynamic model was adopted and integrated with particle dynamic and geochemical submodels. The integrated model was calibrated and applied in a study of the long-term transport and fate of particle-associated contaminants, and polychlorinated biphenyls (PCBs) were used as an example of non-conservative, particle-reactive chemicals. The capability of simulating these chemicals implies that the integrated model can be used to study a wide range of chemicals of natural or anthropogenic origins.

2. Model formulation and integration

2.1. Overview

There are a number of available hydrodynamic and water quality models that can be applied to shallow coastal oceans (Cheng and Casulli, 2001; Cheng et al., 1993; Martin and McCutcheon, 1999; Sheng et al., 1992; Sheng, 1996). For shallow coastal oceans and estuaries, it is essential that the residual currents and baroclinic forcing be reproduced in order to achieve satisfactory accuracy. At the same time, due to the strong influence of tides, the model should also be able to simulate the tidal forcing, and drying–wetting of shallow intertidal zone during flooding and ebbing tides.

Based on the above considerations, a numerical hydrodynamic model, TRIM (representing Tidal, Residual, Intertidal Mudflat Model), was selected in this study because it allows an efficient and accurate simulation of tidal-influenced shallow estuarine environment and has been fully calibrated and verified in San Francisco Bay and San Diego Bay (Cheng et al., 1993; Wang et al., 1998). The model uses a semi-implicit, time-stepping finite-difference numerical method to solve the nonlinear, depth averaged (2-D) shallow water equations. An Eulerian–Lagrangian method (ELM) was used to treat advection terms in the momentum equations such that the numerical method is unconditionally stable if the baroclinic forcing is weak. For many shallow seas, a depth-averaged model is sufficient to simulate the hydrodynamics of shallow water circulation accurately and efficiently. The model also keeps track of drying and wetting of shallow water cells during flooding and ebbing tides, making it an ideal choice for hydrodynamic modeling of tidal shallow coastal environments.

The integrated model was formulated by combining the newly designed geochemical and particle dynamic modules with the original TRIM model. The additional modules provide functionalities such as sediment resuspension, partitioning of chemicals between aqueous and

particle phases, particle settling, storm events, river input of freshwater, and evaporation. These functionalities were implemented in the form of individual subroutines in the computer program of the original TRIM model. The so-called geochemical and particle dynamic submodels were in effect conceptualized units consisting of one or more of the above subroutines. The geochemical submodel was embedded in the partitioning subroutine, and particle dynamic submodel consisted of subroutines that simulate tidal resuspension, particle settling, and some random processes (storms, shipping activities, etc.) that affect SPM concentrations. Details of the integrated model are given below.

2.2. Hydrodynamic submodel

The hydrodynamic submodel performs the simulations of tides (i.e. variations in water surface elevation) and tidal/residual circulations. The governing equations include the conservation equations of mass, momentum, conservative scalar variables, and an equation of state (Cheng et al., 1993). In Cartesian coordinates, the depth averaged continuity equation (i.e., conservation of mass) is given by

$$\frac{\partial \zeta}{\partial t} = \frac{\partial[(h+\zeta)U]}{\partial x} + \frac{\partial[(h+\zeta)V]}{\partial y} = 0 \tag{1}$$

the x-momentum equation (conservation of momentum at x-direction) by

$$\frac{\mathrm{D}U}{\mathrm{D}t} - fV = -g\frac{\partial \zeta}{\partial x} + \frac{1}{\rho_0(h+\zeta)}\left(\tau_x^{\mathrm{w}} - \tau_x^{\mathrm{b}}\right) + A_{\mathrm{h}}\nabla^2 U - \frac{g}{2\rho_0}(h+\zeta)\frac{\partial \rho}{\partial x} \tag{2}$$

the y-momentum equation (conservation of momentum at y-direction) by

$$\frac{\mathrm{D}V}{\mathrm{D}t} - fU = -g\frac{\partial \zeta}{\partial y} + \frac{1}{\rho_0(h+\zeta)}\left(\tau_y^{\mathrm{w}} - \tau_y^{\mathrm{b}}\right) + A_{\mathrm{h}}\nabla^2 V - \frac{g}{2\rho_0}(h+\zeta)\frac{\partial \rho}{\partial y} \tag{3}$$

a scalar transport equation by

$$\frac{\mathrm{D}C_i}{\mathrm{D}t} = \frac{1}{(h+\zeta)}\nabla[K_{\mathrm{h}}(h+\zeta)\nabla C_i] + \sum(I_i) + \sum(O_i) \tag{4}$$

and an equation of state,

$$\rho = \rho_0[1 + (0.78C_0 - 0.75)/1000] \tag{5}$$

Density is treated as a function of salinity (C_0) only. In the temperature range of 10−20 °C, the temperature dependence of water density can be neglected (Cheng et al., 1993). For the definitions of the symbols, please refer to Table 1.

Table 1
Definitions of symbols

Symbol	Definition
A	Atmospheric input
A_{h}	Horizontal eddy viscosity coefficient
C_i	General representation of the concentration of a chemical of interest
C_{oc}	Organic carbon normalized concentration of particulate phase PCB in ng/kg
C_{p}	Particle phase PCB concentration in ng/kg
C_{w}	Dissolved phase PCB concentration in ng/L
C_{we}	Equilibrium dissolved phase PCB concentration in ng/L
C_z	Chezy coefficient used in calculation of bottom shear stress
D	Diameter of the particulate matter in ìm in Sternberg's scheme
$\frac{\mathrm{D}}{\mathrm{D}t}$	$\frac{\mathrm{D}}{\mathrm{D}t} = \frac{\partial}{\partial t} + U\frac{\partial}{\partial x} + V\frac{\partial}{\partial y}$ is the substantial derivative in the x–y plane, which is the time rate of change of a property following a fluid particle (i.e. a Lagrangian concept) in an Eulerian coordinate system
f	Coriolis parameter
f_{oc}	Fraction of organic carbon in the particulate phase
g	Gravitational acceleration
h	Reference water depth at mean lower low water
H	Total water depth ($h+\xi$)
K_{h}	Horizontal diffusivity coefficient
K_{oc}	Organic carbon normalized particle–water partition coefficient
K_{ow}	Octanol–water partition coefficient
n	Manning's constant used in Manning–Chezy equation
OC	Percentage of organic carbon in SPM
R	River input of PCB
S_{d}	Amount of SPM settling in mg/L
S'_{d}	Loss of particulate PCB due to settling
U, V	Depth averaged velocity components at x, y directions
$\vec{U}$	Vector linear velocity of the water mass
W_{s}	Settling speed in mm/s calculated following Sternberg's scheme
(x, y, z)	Cartesian coordinates
Δt	Length of the time step
$\Delta_{\mathrm{w-p}}$	Amount of PCB adsorption in ng/L
Φ	Overall mass discharge across a designated cross section
ε	Amount of resuspension in mg/L
ε'	Addition of particulate PCB due to sediment resuspension
λ	Biodegradation/chemical transformation rate constant (s^{-1})
ρ	Depth averaged water density
ρ_0	Reference density of water
τ_{ce}	Critical shear stress for sediment resuspension
τ_{d}	Critical bottom shear stress for sediment settling
τ_x^{w}, τ_y^{w}	Specific wind stress
τ_x^{b}, τ_y^{b}	Bottom shear stresses
ζ	Free-surface above a reference horizontal plane (MLLW)
∇	$\nabla = \boldsymbol{i}\frac{\partial}{\partial x} + \mathbf{j}\frac{\partial}{\partial y}$ is a vector operator in x–y plane

In Eqs. (2) and (3), the terms starting from the left are the substantial derivatives of U and V, the momentum flux due to Coriolis acceleration, difference in water surface elevation (propagation of gravity waves), wind and bottom shear stress, turbulent dispersion of momentum, and baroclinic change of momentum flux. The salt transport equation, Eq. (4), is needed only if $\frac{\partial \rho}{\partial x}$ and $\frac{\partial \rho}{\partial y}$ are not zero in Eqs. (2) and (3), i.e., the baroclinic condition exists. The conventional Manning–Chezy type of formulation is used for the bottom shear stresses such that

$$\tau_x^b = \frac{\rho_0 g U \sqrt{U^2+V^2}}{C_z^2}, \quad \tau_y^b = \frac{\rho_0 g V \sqrt{U^2+V^2}}{C_z^2} \tag{6}$$

where C_z is the Chezy coefficient relating to a Manning's constant n by (Cheng et al., 1993)

$$C_z = \frac{(h+\zeta)^{1/6}}{n} \tag{7}$$

In the model, a series of n values were assigned for computation cells of different depth (Wang et al., 1998). With appropriate boundary and initial conditions, Eqs. (1)–(6) constitute a well-posed initial-boundary value problem whose solution describes the depth-averaged circulation in a tidal basin.

2.3. Particle dynamics submodel

The particle dynamic submodel in the integrated model simulates processes of resuspension and settling of SPM. In the water column, SPM was treated as an aqueous chemical species. For SPM, the source and sink terms in Eq. (4) became resuspension and settling, respectively:

$$\sum(I_i) = \varepsilon_i, \tag{8a}$$

$$\sum(O_i) = S_{d,i} \tag{8b}$$

where the subscript i denotes particle size group, ε is the amount of particles resuspended during each time period Dt in mg/L; S_d is the amount of settled particles during Dt in mg/L (Table 1). In most cases, SPM concentrations were generally low enough (<10 mg/L) that their effect on the water density ($<10^{-5}$) can be neglected. As the computation of terms other than ε and S_d is carried out by the hydrodynamic model, particle dynamics simulation is simplified to modeling sediment resuspension and settling. Following the scheme proposed by Partheniades (1965), sediment resuspension for the ith group can be determined by the relationship between the bottom shear stress (τ_b) and 'critical shear stress' for erosion (τ_{ce}):

$$\varepsilon_i = \frac{M_{ce}}{(h+\zeta)}\left(\frac{\tau_b}{\tau_{ce.i}} - 1\right) \quad \text{if } \tau_b > \tau_{ce,i} \tag{9a}$$

$$\varepsilon_i = 0 \quad \text{if } \tau_b < \tau_{ce,i} \tag{9b}$$

where M_{ce} is an empirical constant (1.0×10^{-4} mg/L). $\tau_{ce,i}$ is an empirical parameter for particle species i. The determination of values of $\tau_{ce,i}$ can only be carried out in the model calibration. The particle settling parameter, S_d, is calculated by (McDonald and Cheng, 1994)

$$S_{d,i} = -\frac{2W_{s,i}}{h+\xi} C_i \left(1 - \frac{\tau_b}{\tau_{cd,i}}\right) \quad \text{if } \tau_b < \tau_{cd,i} \tag{10a}$$

$$S_{d,i} = 0 \quad \text{if } \tau_b > \tau_{cd,i}, \tag{10b}$$

where $\tau_{cd,i}$ is the critical bottom shear stress for deposition for the ith particle species, which is a threshold bottom shear stress allowing sediment to deposit on bed. Like $\tau_{ce,i}$, $\tau_{cd,i}$ will also be determined in model calibration; $W_{s,i}$ is the settling velocity (mm/s) calculated following the method of Sternberg et al. (1999) as

$$W_{s,i} = 0.0002 D_i^{1.54} \tag{11}$$

where D_i is the diameter of the ith particle species in μm.

As will be seen later, the success of the integrated modeling is dependent heavily on the simulation of particle dynamics, which is the crucial link between hydrodynamic model and geochemical model. It is also a complicated issue in that it requires quantification of many empirical constants through testing and calibration. As stated above, the equations for resuspension and settling of particles are for two specific particle sizes only. If a more robust particle dynamic modeling is desired, additional particle sizes should be integrated into the model. However, the calibration of such model would be challenging due to the requirement of a large amount of observational data on particle sizes as well as characterizations of each size group (e.g. TOC, density, etc.). At the same time, the empirical parameters in Eqs. (9a), (9b), (10a), (10b) and (11) may need to be calibrated individually for each size group. As a result, a balance needs to be struck between model performance and simplicity.

2.4. Geochemical submodel

The geochemical submodel simulates the transport and fate of chemical species with hydrodynamic and particle dynamic processes. It was designed to simulate the transport and geochemical behavior of non-

conservative, hydrophobic chemicals. Following the general form of the transport equation (Eq. (4)), the source and sink terms for the chemical species in the dissolved and particulate phases are (see Table 1 for definitions of the symbols):

Dissolved phase:

$$\sum(I_{w,i}) + \sum(O_{w,i}) = -\lambda C_{w,i} - \Delta_{w-p} + A_{w,i} \quad (12)$$

Particulate phase:

$$\sum(I_{p,i}) + \sum(O_{p,i}) = -\lambda C_{p,i} + \Delta_{w-p} + A_{p,i} + \varepsilon' - S_d' \quad (13)$$

Eqs. (12) and (13) indicate that the capabilities of the chemical submodel include but are not limited to the following processes: Biodegradation/chemical transformation, adsorption/desorption, atmospheric input, input and output due to particle resuspension and settling. Obviously, more source and sink terms can be added for chemicals that are subject the corresponding processes; for conservative chemicals there will be no source and sink terms.

Finally, the net flux of the i-th chemical species (Φ_i) across any given cross section in the model domain can be calculated by (see Table 1 for definitions of the symbols)

$$\Phi_i = \sum_{j=1}^{N} \left\{ \left[\sum_{k=1}^{M} \vec{U}(k) * dy * H(k) * C_i(k) \right] * \Delta t_j \right\} \quad (14)$$

where N is the number of time steps used, and M is the number of cells on the cross section.

3. Application of the integrated model in San Diego Bay

3.1. Overview

The integrated geochemical and hydrodynamic model was applied in a study of polychlorinated biphenyls (PCBs) in San Diego Bay (SDB), California, a semi-closed embayment on the southwestern corner of California near the US–Mexico border (Fig. 1). It covers an area of about 4.1×10^7 m^2 at mean lower low water with an average depth of about 6.5 m (Chadwick et al., 1999). In general, north SDB is narrow and deep and south SDB is broad and shallow, with a large stretch of intertidal mudflat at the southern end. It is a typical low-inflow estuary with an annual precipitation of about 25 cm and excess evaporation of up to 160 cm in dry season. The semidiurnal tides in the bay have an average range of 1.7 m with maximum tidal amplitudes of about 3 m (Chadwick et al., 1999). Bordered by four cities including the City of San Diego with an estimated total population of 1.2 million, SDB is used by a large number of recreational, commercial, and naval facilities. Heavy commercial and military shipping activities and surface runoff draining densely populated areas have resulted in highly elevated levels of organic contaminants and metals in sediments and biota (Chadwick et al., 1999; Chadwick et al., 2004; Zeng et al., 2002). Of particular concern to the environmental management community is the widespread distribution of PCBs in sediments and biota within SDB. These studies implicated the sediments of historical 'hot spots' as the main source of PCBs in the water column of SDB (Chadwick et al., 1999; Fairey et al., 1998; McCain et al., 1992; Noblet, 2002; San Diego Bay Interagency Water Quality Panel, 1994; Zeng et al., 2002). Sediment-bound PCBs can be released to the water column through sediment–water interaction and during sediment resuspension. Subsequently, PCBs in the water column are then transported to the open ocean through tidal exchange, which also brings cleaner water from the open ocean. We measured concentrations of individual PCB congeners at stations 1–9 (see Fig. 1) during summer 1999 and winter 2000 (Zeng et al., 2002), and the data are presented in Table 2.

Due to tidal exchange, the average residence time for waters within SDB is estimated to be only 11 days, and as short as 1 day at the bay mouth (Chadwick et al., 2004; Largier, 1995). Obviously, there are large variations in hydrographical conditions as well as in the concentrations of many environmentally significant chemicals due to vigorous tidal exchange. As a result, to obtain information of these chemicals, spatial distributions or 'snap shots' are not sufficient. On the other hand, comprehensive investigations involving time-series observations and measurements throughout the study area are often too costly. For example, tidal variations in SDB consist of semidiurnal, biweekly, and 6-month components. As a result, the observation data need extrapolation and interpolation in both spatial and temporal scales. However, lack of observational data in some areas makes extrapolation or interpolation difficult.

Based on the above considerations, the integrated model as described previously was used. The hydrodynamic submodel has been calibrated and verified in SDB (Wang et al., 1998). In order to run the model efficiently on personal computers for long-term simulations (>100 days), the grid size was changed to 150×200 m from the original 50×50 m. The length of time step was also optimized to 3 min/step to achieve the

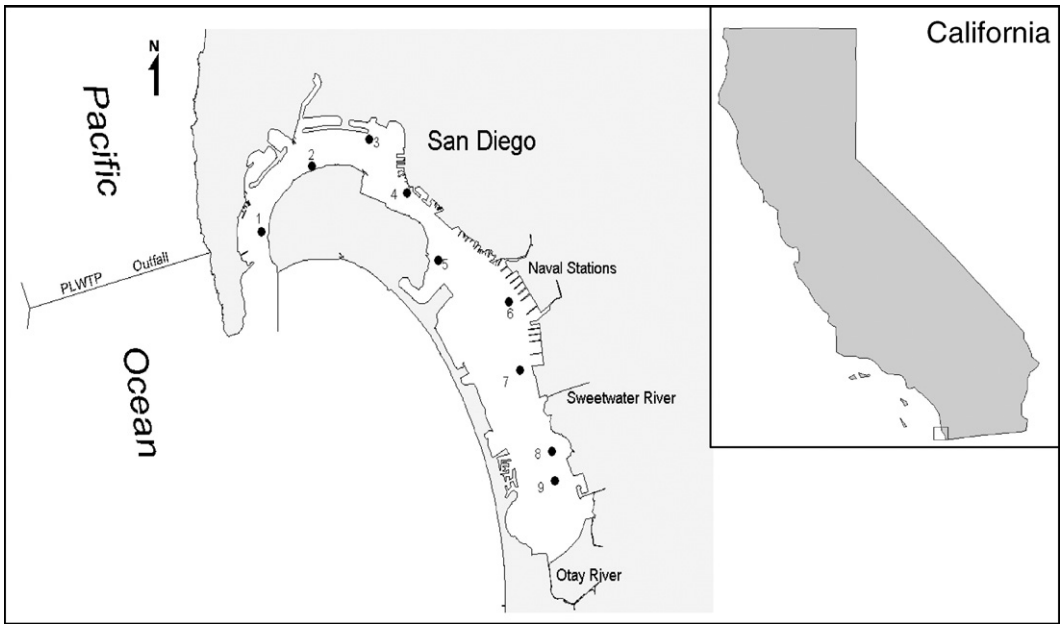

Fig. 1. Map of San Diego Bay showing the sampling locations.

most efficient simulations for the revised grid size without affecting the numerical stability of the model. An evaporation function was added to the original model to extract freshwater from SDB at an average rate of 160 cm/year (Chadwick et al., 1999). The values of salinity and other chemical species in the water column were adjusted accordingly due to evaporation.

In the particle dynamic submodel for SDB, two particle sizes of 2 and 20 μm were used to represent clay and fine silt, respectively. This simplified treatment of suspended particles was necessary for the realistic calibration of the modeling of particle dynamics due to the lack of a complete data set of sediment sizes. The use of only fine particles also corresponds to Eqs. (9a), (9b) and (10a), (10b) that were based on the investigations on cohesive muddy sediments in shallow environments (Christiansen et al., 2000; Lumborg and Windelin, 2003; Martin and McCutcheon, 1999; Partheniades, 1965; Taki, 2001). Lastly, compared to coarse particles, fine particles are more closely associated with organic carbon in both water column (Chadwick et al., 1999) as well as surface sediments (K. Richter, personal communications). Since PCBs interact only with organic portion of the fine particles, the simplified treatment of particle sizes is not expected to significantly affect model performance.

Since the time scale of the simulation (within 1 year) is considerably shorter than that of PCB biodegradation, the λC terms in Eqs. (12) and (13) were neglected in the present study. In addition, the river and atmospheric inputs of PCBs are deemed negligible (Chadwick et al., 1999). The governing equations for geochemical submodel (Eqs. (12) and (13)) can be simplified to

Dissolved phase:

$$\sum(I_{w,i}) + \sum(O_{w,i}) = -\Delta_{w-p} \tag{15}$$

Particulate phase:

$$\sum(I_{p,i}) + \sum(O_{p,i}) = \Delta_{w-p} + \varepsilon' - S_d' \tag{16}$$

The central part of the simulation was the term Δ_{w-p}, i.e. the partitioning of the chemicals between the dissolved and particulate phases. If the partitioning of PCBs between the dissolved and particulate phases is assumed to be at equilibrium, C_w and C_p are related to each other by the organic carbon normalized particle–water partition coefficient (K_{oc}), i.e.,

$$K_{oc} = \frac{C_p}{C_{w,e} \times OC} = \frac{C_{oc}}{C_{w,e}} \tag{17}$$

where $C_{w,e}$ is the dissolved PCB concentration at equilibrium with the particulate phase (see Table 2); C_{oc} ($=C_p/OC$) is the organic carbon normalized PCB concentration in the particulate phase; and OC is the content of organic carbon in the particulate phase. Eq. (17) indicates that if the TSS concentration changes due to resuspension/settling, the concentrations of PCBs in both the dissolved and particulate phases will change

Table 2

Congener	logK_{ow}[a]	1-1m	1-5m	2-1m	3-1m	3-5m	4-1m	4-5m	5-1m	5-5m	5-5m[b]	6-1m	6-5m	7-5m	8-1m	8-5m	9-1m	Average
(a) Observed concentrations of PCB congeners (ng/L) in SDB during summer 1999 sampling season																		
18	5.24	nd	nd	nd	0.0154	0.0156	nd	nm	0.0195	0.0207	0.0131	0.0231	nm	0.0156	nd	0.0100	0.0118	0.0161
28	5.67	nd	nd	nd	0.0152	0.0211	nd	nm	0.0182	0.0177	0.0172	0.0299	nm	0.0133	0.0104	0.0163	0.0107	0.0170
52	5.84	0.0119	nd	0.0101	0.0319	0.0257	0.0212	nm	0.0358	0.0357	0.0352	0.0487	nm	0.0391	0.0247	0.0340	0.0206	0.0288
44	5.75	nd	nd	0.0117	0.0197	0.0187	0.0111	nm	0.0212	0.0267	0.0227	0.0278	nm	0.0192	0.0118	0.0153	nd	0.0187
66	6.20	nd	nd	0.0126	0.0173	0.0159	0.0111	nm	0.0216	0.0200	0.0215	0.0234	nm	0.0162	nd	0.0149	nd	0.0175
101	6.38	0.0133	nd	0.0208	0.0247	0.0252	0.0217	nm	0.0333	0.0324	0.0349	0.0442	nm	0.0352	0.0189	0.0319	0.0171	0.0272
87	6.29	nd	nd	nd	nd	nd	nd	nm	nd	nd	0.0101	0.0134	nm	nd	nd	nd	nd	0.0118
118	6.74	nd	nd	0.0121	0.0134	0.0139	0.0118	nm	0.0158	0.0158	0.0188	0.0223	nm	0.0151	nd	0.0167	nd	0.0156
153	6.92	nd	nd	0.0159	0.0166	0.0246	0.0216	nm	0.0235	0.0156	0.0251	0.0333	nm	0.0215	0.0128	0.0280	0.0109	0.0208
138	6.83	nd	nd	nd	nd	0.0158	0.0117	nm	0.0136	0.0114	0.0129	0.0112	nm	0.0115	nd	0.0155	nd	0.0130
Total		0.025	nd	0.083	0.154	0.177	0.110		0.203	0.196	0.212	0.277		0.187	0.079	0.183	0.071	
SPM (mg/L)		5.00	2.30	8.00	7.80	1.10	2.40		3.00	3.60	5.10	1.90		3.00	6.30	2.00	7.80	
TOC		3.80	2.69	2.93	3.36	2.30	3.23		4.18	3.43	3.28	2.19		4.03	2.40	2.15	3.31	
(b) Observed concentrations of PCB congeners (ng/L) in SDB during winter 2000 sampling season																		
18	5.24	0.0076	nd	0.0111	0.0174	0.0257	0.0136	0.0175	0.0107	0.0113	nm	0.0142	0.0121	nm	nd	0.0119	nd	0.0139
50	5.63	nd	nd	nd	nd	0.0182	nd	nd	nd	nd	nm	nd	nd	nm	nd	nd	nd	0.0000
28	5.67	0.0152	nd	0.0288	0.0412	0.0490	0.0295	0.0428	0.0266	0.0257	nm	0.0209	0.0288	nm	0.0250	0.0220	0.0294	0.0296
52	5.84	0.0136	0.0544	0.0237	0.0423	0.0650	0.0425	0.0432	0.0367	0.0388	nm	0.0347	0.0435	nm	0.0316	0.0334	0.0272	0.0379
44	5.75	nd	nd	0.0124	0.0222	0.0328	0.0196	0.0165	0.0178	0.0169	nm	0.0136	0.0171	nm	0.0133	0.0153	nd	0.0180
66	6.20	0.0094	nd	0.0172	0.0280	0.0368	0.0261	0.0239	0.0255	0.0234	nm	0.0185	0.0271	nm	0.0151	0.0150	nd	0.0222
101	6.38	0.0115	nd	0.0195	0.0329	0.0430	0.0350	0.0278	0.0325	0.0321	nm	0.0311	0.0420	nm	0.0254	0.0221	0.0162	0.0285
87	6.29	nd	nd	0.0055	0.0103	nd	0.0115	nd	0.0093	0.0081	nm	0.0084	0.0112	nm	nd	0.0092		
118	6.74	nd	nd	0.0154	0.0208	0.0272	0.0231	0.0176	0.0207	0.0161	nm	0.0155	0.0219	nm	0.0150	0.0119	nd	0.0187
153	6.92	0.0078	nd	0.0145	0.0205	0.0195	0.0229	0.0191	0.0218	0.0156	nm	0.0172	0.0229	nm	0.0143	0.0145	nd	0.0175
105	6.65	nd	nd	0.0079	nd	nd	0.0080	nd	0.0066	nd	nm	nd	nd	nm	nd	nd	nd	0.0075
138	6.83	nd	nd	0.0149	0.0121	0.0142	0.0134	0.0120	0.0149	0.0096	nm	0.0105	0.0169	nm	nd	nd	nd	0.0132
187	7.17	nd	nd	nd	nd	nd	nd	nd	0.0052	nd	nm	nd	nd	nm	nd	nd	nd	0.0052
180	7.36	nd	nd	nd	nd	nd	nd	nd	0.0050	nd	nm	nd	nd	nm	nd	nd	nd	0.0050
Total		0.065	0.054	0.171	0.248	0.331	0.245	0.220	0.233	0.198		0.184	0.244		0.140	0.146	0.140	
SPM (mg/L)		4.49		3.26	3.05	3.69	3.46		1.28	1.66		1.36	1.90		5.10	5.35	8.44	
TOC		2.34		3.90	5.03	5.75	3.22		3.87	4.18		5.16	4.01		2.70	2.85	2.89	

nd: not detected.

nm: not measured.

[a] Based on Hawker and Connell (1988).

[b] Duplicate samples.

accordingly to maintain a constant K_{oc}. At the same time, the total amounts of PCBs are conserved before and after the re-partitioning.

Practically K_{oc} is not readily available, but it can be associated with the commonly available octanol–water partition coefficient, K_{ow} by

$$\log K_{oc} = a \log K_{ow} + b \quad (18)$$

with a and b determined experimentally.

3.2. Boundary and initial conditions

The hydrodynamic submodel is driven by tides defined by a tidal function on the open boundaries (north, west, and south) of the model domain (Cheng et al., 1993; Wang et al., 1998). The values of the harmonic constants defining the boundary conditions were determined through extensive calibration and verification using data collected in 1983 and 1992−1996 (Wang et al., 1998).

In the particle dynamics submodel, the SPM concentrations at the open boundaries are set to 1 mg/L, which essentially represents the background values observed previously (Chadwick et al., 1999). The initial SPM concentrations for non-boundary cells are assumed to be zero. Of the two particle sizes considered in the present study, only the 2-μm particles are assumed to be present at the open boundaries. The initial value of salinity is set to 33.5 throughout the model domain based on field measurements (Chadwick et al., 1999; Peng, 2004). This value is also always maintained at the open boundaries. After the model spin-up, salinity varies with the mass balance of water and salt, and SPM is produced dynamically until a quasi-equilibrium state is eventually reached. These aspects will be discussed in the following section. Initial PCB concentrations are set to zero at open boundaries and at all water cells except for those 'hot spots', which were assumed to have fixed concentrations of PCBs, as will be discussed in the model calibration.

3.3. Random inputs of freshwater and particulate matter

As an 'urban ocean' environment, SDB is heavily influenced by anthropogenic sources, including shipping activities and storm water runoff that input large amounts of particulate matter into the water column. Runoff also brings in a fair amount of freshwater in the bay. The quantitative levels and randomness of these inputs need to be modeled adequately in the simulation.

To simulate the effects of shipping activities, the data from a 2-month survey of suspended particles revoked by U.S. Navy warships were used (Chadwick et al., 1999). The randomness of these shipping events was controlled by a series of random numbers generated in each time step. River inputs of particulate matter and freshwater were simulated for two major rivers, Sweetwater River and Otay River (Fig. 1). Based on the drainage area (970 km^2) of SDB, average rainfall (25 cm/year), and an assumed average land retention factor (70%), the amount of freshwater flow into SDB could be estimated. Computer-generated random numbers were used to simulate major, average, and minor rainfalls with 5, 2.5, and 1 cm of precipitation, respectively. The frequency of these precipitation events was prescribed by the random numbers such that on average 25 cm of precipitation was produced each year. The duration of each precipitation event was assumed to be 12 h. Finally, the SPM content of river inflow was 60 mg/L, a number consistent with a previous measurement (Chadwick et al., 1999).

4. Model calibration

The calibration and validation of the hydrodynamic model in SDB were already carried out with satisfactory results (Cheng et al., 1993; Wang et al., 1998), so they are not repeated here. The calibration and validation of the geochemical and particle dynamics submodels were based on long-term simulation that lasted 104 days and ended in mid-June of 1999 when the first field sampling was conducted. The concentrations of the chemical species were found to have reached dynamic equilibrium within 15 days.

4.1. Freshwater input calibration

Salinity is an excellent indicator for the model calibration because it is a conservative chemical tracer. It provides a strong constraint upon the amount of freshwater input from rivers, thus ensuring a good simulation of the dilution or accumulation of other chemicals in the water column in SDB. Without proper calibration of the freshwater input, the model would produce severe 'pumping' effects for some man-made chemicals in south SDB, such as sustained high concentrations of PCBs that was inconsistent with observation (Zeng et al., 2002).

Freshwater inputs from Sweetwater River and Otay River (see Fig. 1 for locations) were difficult to estimate because of sporadic surface flow and constraints exerted by the river dams during wet weather season (Fig. 2). On

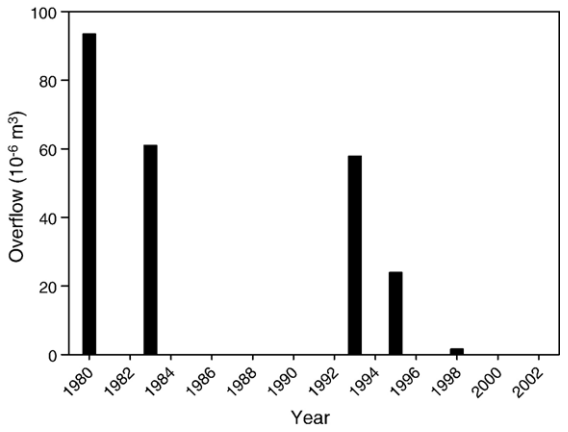

Fig. 2. Records of flow in acre-feet over Sweetwater Dam since 1980 (courtesy of Michael Garrod of Sweetwater Authority).

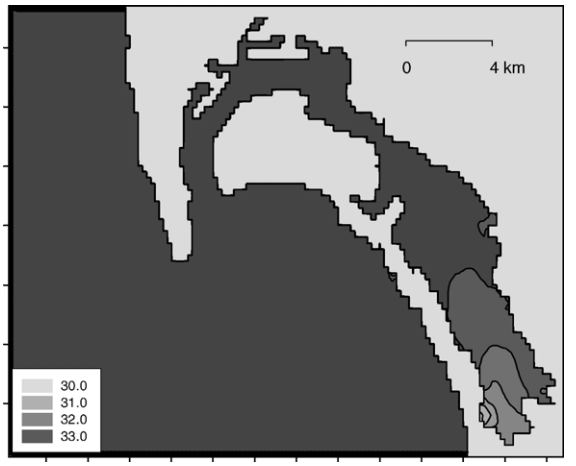

Fig. 3. Simulated salinity distribution in SDB with a retention ratio of 70%. Hypersaline condition is missing. This implies that the retention ratio is too low (too much fresh water is input to SDB).

the other hand, initial model calibrations indicated that the actual amount of freshwater input was a crucial parameter for the integrated model, especially in the simulation of chemical species. In SDB, low salinity and slightly hypersaline conditions are typical during the wet and dry weather seasons, respectively (Chadwick et al., 1999; Largier et al., 1997). During two sampling cruises in summer 1999 (dry weather season) and winter 2000 (wet weather season), the measured salinities were in a narrow range of 32−35. Higher (up to 37) and lower (~25) salinity values have also been reported during a prolonged dry period and after major precipitation, respectively (Chadwick et al., 1999; Largier et al., 1997). The calibration of the model in terms of freshwater inflow and salinity pattern requires long-term (at least 3 months) simulations due to the slow evaporation rate compared to the volume of SDB. The results consistently showed that the amount of freshwater input to SDB was much smaller than the assumed retention factor of 70%. Obviously, the difference reflects the restriction of freshwater inflow by the river dams. Simulations employing a retention factor of 70% yielded lower salinity values in south SDB than other parts of SDB (Fig. 3), inconsistent with observed patterns (Chadwick et al., 1999; Largier et al., 1997; Peng, 2004). In contrast, calibrations with a retention factor of 85% resulted in salinity values compatible with the observation, as shown in Fig. 4.

4.2. SPM calibration

As stated previously, the amount of sediment resuspended in the water column due to tidal currents can be predicted via the particle dynamics submodel. The critical bottom shear stress for erosion, τ_{ce}, and critical shear stress for deposition, τ_{cd}, are two important empirical parameters used to describe resuspension and settling of particles, respectively (Eqs. (9a), (9b) and (10a), (10b)). Previous studies on environments similar to SDB obtained τ_{ce} in the range of 0.1−0.5 N/m^2. The τ_{cd} value is typically around 0.01 N/m^2 (Christiansen et al., 2000; Krone, 1962; Lumborg and Windelin, 2003; Partheniades, 1965; Sternberg et al., 1999; Torfs et al., 2001; van Rijn, 1989).

Human-induced sediment resuspension complicated the calibration process in SDB. If shipping-induced resuspension were not considered, calibration runs

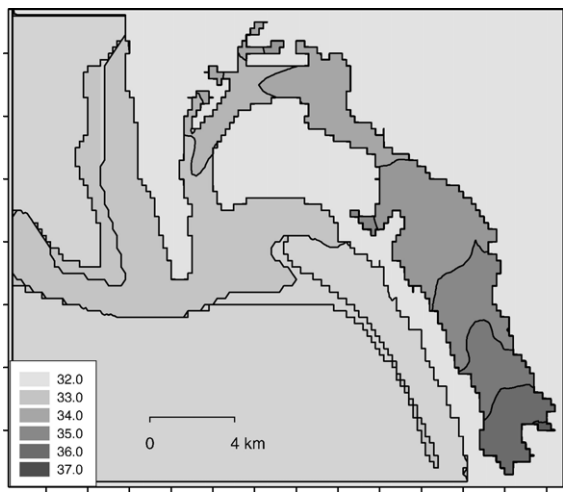

Fig. 4. Simulated salinity distribution in SDB using a retention ratio of 85%. Generally observed hypersaline condition (Hawker and Connell, 1988) is realistically reproduced. In all subsequent simulations, retention ratio of 85% will be used.

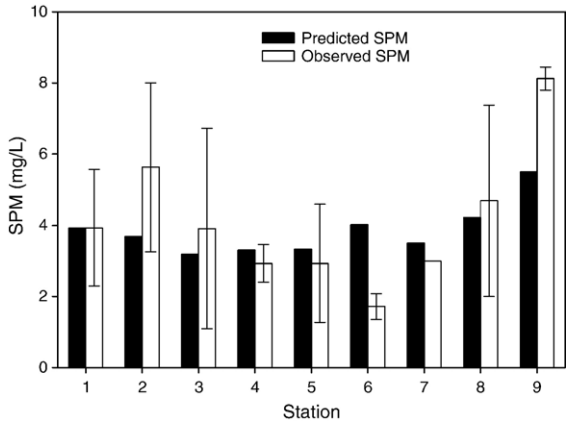

Fig. 5. Comparison between the predicted and observed concentrations of SPM (mg/L). Vertical bars for the observed values indicate the error ranges of the field data.

showed that tidal currents would produce less than half of the observed SPM concentrations in the water column. Therefore, the impact of shipping events had to be adequately simulated in order to reproduce the observed SPM patterns. The optimal values of τ_{ce} determined from fitting the predicted and observed TSS values were 0.1 and 0.12 N/m^2 for the particle sizes of 2 and 20 μm, respectively. Similarly, the optimal values of τ_{cd} for the particle sizes of 2 and 20 μm were 0.02 and 0.05 N/m^2, respectively.

The model predicted SPM concentrations were in general agreement with the measured values (Fig. 5). There is a large range for observed values, presumably due to patchiness of suspended sediment distribution. The simulated SPM levels generally fall within the range of the observed values, with a small (5.9%) difference between the average values. Hence, the simulation of the TSS distribution in the water column of SDB by the model was deemed satisfactory.

4.3. PCB calibration

Previous studies by U.S. Navy and other agencies on the sediment PCB contamination around SDB showed that highest contamination levels are centered at the submarine base near the eastern end of Coronado Bridge, and near the Cruise Ship Terminals (Chadwick et al., 1999; SDSC, 2004), so they are probably the chief sources of PCBs in SDB. Sediment PCB concentrations at other locations within SDB were all near or below detection limit. There has been evidence that persistent organic contaminants can diffuse into the water column, thus becomes the chief source of the contaminants when the sediment concentration of this contaminant is high (Zeng et al., 1999). This could probably be the case in SDB, where sediments at some 'hot spots' with very high concentrations (>1500 ppb) of PCBs provide continuous source of PCB into the overlying water column. Fig. 6 shows a close resemblance between the 'fingerprints' of the concentrations of PCB congeners in water column and sediment at the above 'hot spots'. More heavily chlorinated PCB (those with higher K_{ow} values) congeners tend to bind to sediment, as shown by a slight difference in the trend lines in Fig. 6. Therefore, it is reasonable to assume that these 'hot spots' are the sources of dissolved phase PCBs in SDB waters. In the model, the input of PCBs is simulated by defining boundary conditions at certain locations that are known to have high PCB concentrations in sediments. Since the sediment–water exchange of PCBs should be a slow process, PCB concentrations in the water column at 'hot spots' should be relatively constant, warranting fixed value boundary conditions for the model.

The initial conditions of PCB concentrations in the particulate phase are not set. Rather, they are simulated dynamically based on SPM levels, TOC and dissolved phase PCBs in the scheme described by Eqs. (15)−(18). Obviously the simulation of PCBs (especially the ratio between PCB concentrations in the dissolved and particulate phases) will be affected by the choice of parameters related to the PCB–particle interactions, or a and b in Eq. (18). Empirical relationship given by Karickhoff et al. (1979) (a=1.0, b=−0.21) was found to fit the observation data better, but significant adjustment was needed in order to fit predictions with observation in terms of the dissolved and particulate

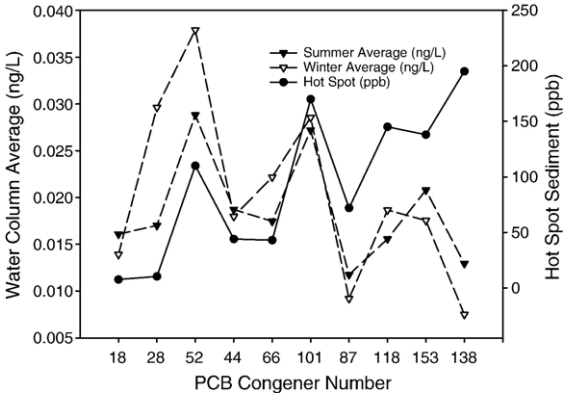

Fig. 6. Comparison between concentrations of dissolved PCB congeners in water columns and sediments. Water column concentrations for individual congeners were averaged for stations 1–9 across SDB. Sediment data was based on Largier et al. (1997). Similar patterns between water column and sediment suggest that water column PCBs may come from sediment through diffusion and resuspension.

phase at the same time. The best result was obtained when $b=-0.51$ was used. On the other hand, the empirical relationship given by Schwarzenbach and Westall (1981) ($a=0.72$, $b=0.49$) was apparently not supported by our model. Using the latter scheme, there are significant overestimates for the concentrations of dissolved phase PCBs, and underestimates for the particulate phase. There have been reports (Cornelissen and Gustafsson, 2005; Cornelissen et al., 2005a; Cornelissen et al., 2005b; Sobek et al., 2004) that elemental carbon (black carbon, char, soot, etc.) in sediment could affect the sorption property such that the linear relationship between K_{oc} and K_{ow} could be altered significantly. However, our previous study (Zeng et al., 2002) did not find effects of elemental carbon on the sorption characteristics of PCBs, thus elemental carbon was not considered in the model. It is cautioned that when this model is applied to other regions, effects of elemental carbon on hydrophobic chemicals need to be carefully evaluated.

When $a=1.0$ and $b=-0.51$ were used in the long-term calibration (~100 days), optimal results were obtained for both dissolved and particulate PCBs (Fig. 7a and b). The predicted spatial distributions of PCBs in the dissolved and particulate phases are shown in Fig. 8a and b. On average, the differences between predicted and observed concentrations are within 10% and 50% for the dissolved

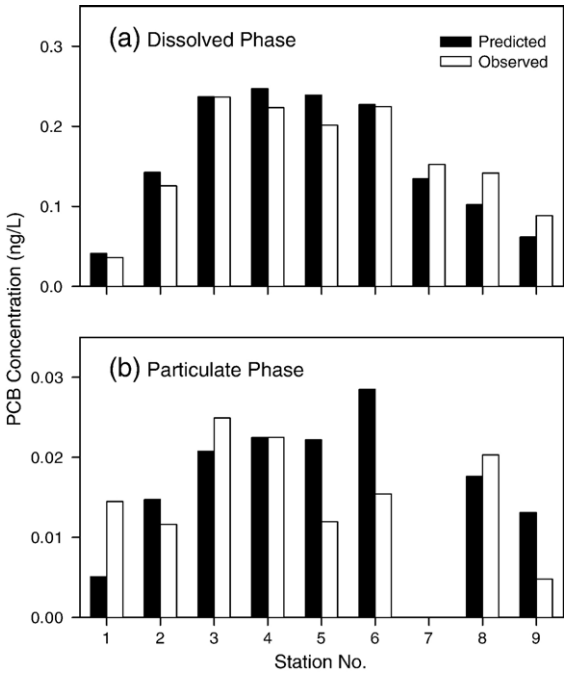

Fig. 7. Comparison between the predicted and measured PCB concentrations in the (a) dissolved phase and (b) particulate phase. Predicted values were based on a 2-day average.

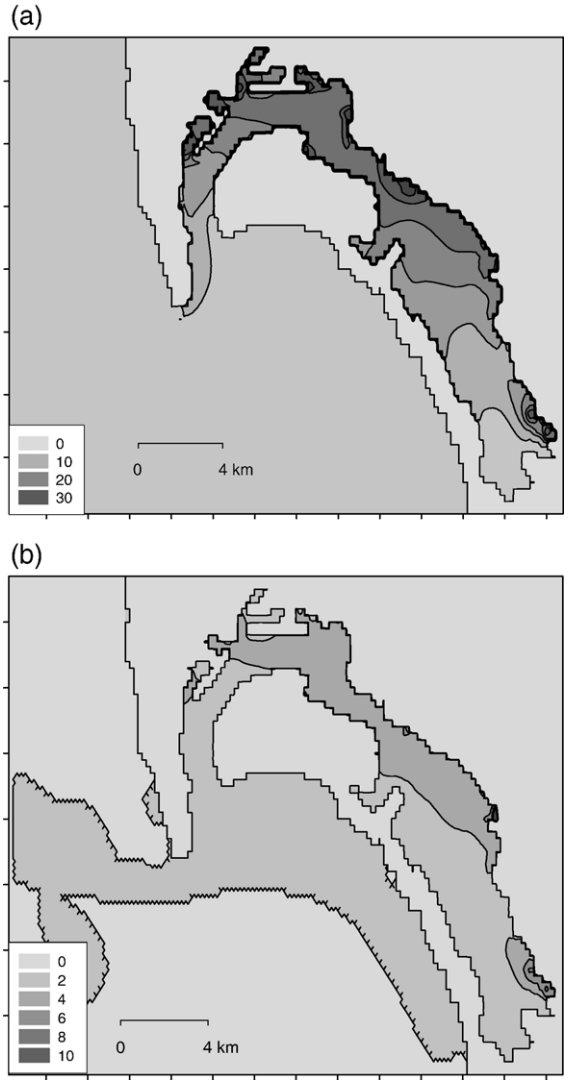

Fig. 8. Simulated steady-state distributions of PCBs in dissolved (a) and particulate (b) phases.

and particulate phase, respectively. If averaged over all stations, the differences between the concentrations of the predicted and observed PCBs in both phases are within 5%. Larger discrepancies for particle phase PCBs were probably due to transient changes in SPM concentrations caused by natural and man-made sediment resuspension. Freshly resuspended particles may not reach equilibrium with the ambient seawater due to insufficient time. Relatively large analytical uncertainties for PCB concentrations, especially for the particulate phase due to their low concentrations, may also have played a role. Uncertainties of the exact locations of the PCB 'hot spots' can also contribute to the differences. For example, the predicted PCB concentrations at south SDB in both phases tend to be lower than observed values, suggesting

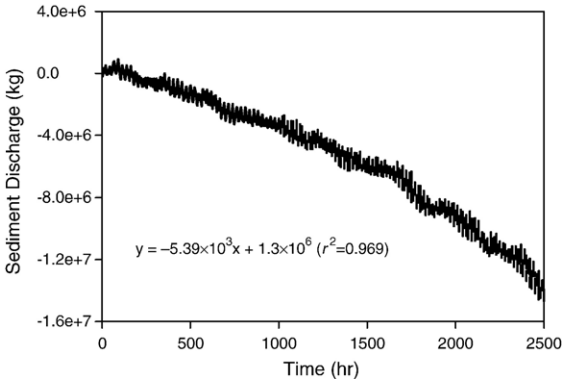

Fig. 9. Simulated mass discharge of suspended sediments (including both the 2 and 20 μm particle sizes) out of SDB. Based on the slope of the curve, the sediment flux was estimated at 4.72×10^7 kg/year ($r^2=0.968$).

that there might be additional 'hot spots' in the south bay that were not fully accounted for in the model. Overall, the calibration of PCBs in both phases is deemed satisfactory and will be applied in the subsequent investigations.

5. Model applications

5.1. Sediment transport simulation

As stated above, SPM was treated as a chemical species once its sources and sinks were properly defined by particle dynamics. Therefore, Eq. (14) can be used to calculate the export of sediment out of SDB when we set the cross section at the bay mouth. The result (Fig. 9) shows that the annual net transport of sediment (a combination of particle sizes of 2 and 20 μm) from SDB to the ocean is 4.72×10^7 kg/year. It is interesting to note that the amount of sediment input from rivers is only 2.25×10^7 kg/year. The discrepancy is a clear indication that river input contributes only part of the suspended fine particles in SDB. Large amount of fine particles are either input from non-point sources such as storm runoff, or produced *in situ* from sediment resuspension due to human activities and tidal currents. The excess of sediment loss over input to SDB does not necessarily suggest that SDB is no longer accumulating sediment since only fine particles are considered in the model. Relatively large ranges in the measurement of SPM concentrations might also be a factor in the apparent sediment imbalance. The discrepancy may be compensated by coarser sediments, which are transported by rivers and storm runoff into SDB but could not be carried out to the open ocean. A comprehensive, long-term sediment transport observation campaign for sediment transport is needed in order to provide better constraints for the integrated model, but it is beyond the scope of the current study.

5.2. Transport and fate of PCBs

Successful calibration of PCB concentrations in both the dissolved and particulate phases lent confidence to the investigation of the transport and fate of PCBs in SDB. Based on Eq. (14), the losses of PCBs and particulate matter across the SDB mouth were calculated. Fig. 10a and b show the net losses of PCBs and particulate matter, which amount to 3.50 kg of PCBs each year in the dissolved form and 0.35 kg in the particulate form. The total loss of PCBs of 3.85 kg is significantly higher than the previous estimate of ~1.0 kg (Zeng et al., 2002), which was based on a residence time of 11.8 days and about 50% reflux of bay water during flooding tides (i.e. about 50% of water flowing into SDB is 'old' SDB water) according to Largier (1995). The difference between these two estimates could come from the following sources: (a) overestimated residence time and reflux ratio by Largier (1995); (b) the use of average concentration of PCBs in the previous calculation (Zeng et al., 2002). In reality,

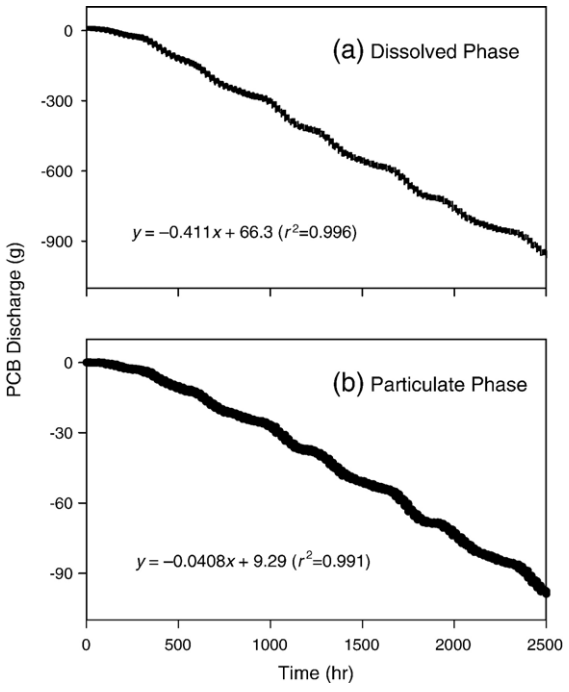

Fig. 10. Simulated mass discharge of PCBs out of SDB in the (a) dissolved phase and (b) particulate phase. Based on the slopes of the curves, fluxes of PCBs of 3.5 ($r^2=0.996$) and 0.35 kg/year ($r^2=0.991$) in the dissolved phase and particulate phase, respectively, were obtained.

north-central SDB sustains more vigorous tidal exchange and it also has relatively higher PCB concentrations. In a dynamic modeling approach as employed in this study, the details of PCB distribution and its transient variations were included implicitly in the numerical model. Therefore, the present calculation should be a better estimate.

6. Discussion

The present study represents an attempt to link hydrodynamics with the resuspension, transport and deposition of suspended solids, enabling it to investigate the transport and fate of environmentally significant chemicals in dynamic coastal environments. The quantitative investigations based on the numerical model are superior to the semi-quantitative estimates based on steady-state assumptions. The integrated model is the first of its kind that explicitly links hydrodynamics, particle dynamics, and geochemistry to study environmental issues. It also has the potentials to study many other chemical species of environmental significance. It is worth mentioning that the model has been applied to naturally occurring, particle reactive radionuclides ^{210}Pb, ^{210}Pb and ^{234}Th in San Diego Bay (Peng, 2004). The model was calibrated with observed concentrations of suspended particles as well as the radionuclides, which provided strong constraints for the geochemical submodel because their natural occurrences are better defined than man-made contaminants. The capability of modeling a diverse range of chemicals testified the value of the integrated model in the studies of geochemical cycles of non-conservative chemicals in dynamic coastal oceans.

A properly calibrated numerical model can help extrapolate and interpolate the field data to the areas not sampled, thus facilitating the data interpretation and visualization by providing a complete and dynamic characterization of the study area. It can also derive secondary information such as the fluxes of water, dissolved chemical species, and SPM, and forecasting and nowcasting of oceanic conditions and chemical distributions. The model can also provide important insights into the 'what-if' scenarios. For example, what environmental consequences would be if certain events (e.g. oil spills, storm runoffs) take place.

The requirement for large quantity of observational data for model setup and calibration can be a limiting factor for the application of the model. In the present study, the hydrodynamic submodel in the integrated model is benefited from years of extensive work (Cheng et al., 1993; Wang et al., 1998), but some components in the sediment dynamics and geochemical submodels are limited by difficulties in obtaining large quantities of data. For example, shipping-induced sediment resuspension is difficult to quantify and predict; river input is so severely affected by reservoirs that vital correlation between precipitation and freshwater input into SDB no longer exists; the number of measurements for PCBs is limited by cost and manpower. Therefore, more observational data are desired to strengthen the geochemical submodel such that the applications of the integrated model can be further explored with more confidence.

The integrated geochemical and hydrodynamic model developed in the present study can be applied to other chemicals and in other study areas. The bathymetry of the study area needs to be obtained, so are the tidal function and large-scale oceanic circulation patterns, which are necessary boundary conditions for the hydrodynamic submodel. Grid dimensions and length of time step for integration need to be optimized for computation efficiency and accuracy. The particle dynamic and geochemical submodels are not as site-specific as hydrodynamic submodel, but careful calibrations pertaining to the specific location (e.g. those with regard to human-induced sediment resuspension; bottom sediment type, etc.) are indispensable. Special attention is needed to treat the interactions between the chemical species and SPM if the chemicals are associated with SPM or components of SPM such as organic carbon or elemental carbon. Observations should also be made on SPM distribution and variation in order to determine the site-specific empirical parameters (i.e. those in Eqs. (9a), (9b), (10a), (10b) and (11)). Long-term calibrations are needed to verify the submodels before the integrated model can be applied.

The present study has provided a framework for the study of environmental issues in tidal coastal oceans and estuaries based on an explicit link between hydrodynamics, particle dynamics, and chemistry of organic and inorganic chemicals. Despite its limitations, it represents an improvement from traditional geochemical studies that are based on steady state assumptions.

Moreover, the modeling approach facilitates visualization and integration of observation results such that inventories and fluxes of chemical species (including SPM) can be quantitatively studied, making it a useful tool to study the transport and fate of environmental pollutants in the coastal seas and estuaries.

Acknowledgement

The modeling work was made possible by the author of the original TRIM model Dr. Ralph Cheng, who offered the TRIM source code and provided insightful

comments on the manuscript. Dr. Teh-Lung Ku of the University of Southern California (USC) encouraged and supported the modeling effort. We thank the crew of the research vessels Metro and Monitor II (City of San Diego) for sampling assistance in San Diego Bay. Special thanks go to Dario Diehl of SCCWRP for managing all field samplings. P.-F. Wang and K. Richter of Space and Naval Warfare System Command (SPAWAR), US Navy are appreciated for their help on the modeling effort and discussions of the manuscript. This study was funded in part by the USC Sea Grant Program, National Oceanic and Atmospheric Administration (NOAA), under Grant CE-5. The USC Sea Grant Traineeship also provided financial support for J.P. during 1999–2001. Support of E.Y.Z. by the "Hundred Talents" Program of the Chinese Academy of Sciences is gratefully acknowledged.

References

Chadwick, B., et al., 1999. Sediment Quality Characterization, Naval Station San Diego, Final Summary Report. SPAWAR, San Diego.

Chadwick, D.B., Zirino, A., Rivera-Duarte, I., Katz, C.N., Blake, A.C., 2004. Modeling the mass balance and fate of copper in San Diego Bay. Limnology and Oceanography 49 (2), 355–366.

Cheng, R.T., Casulli, V., 2001. Evaluation of the UnTRIM model for 3-D tidal circulation. 7-th International Conference on Estuarine and Coastal Modeling, St. Petersburg, Fl, pp. 628–642.

Cheng, R.T., Casulli, V., Gartner, J.W., 1993. Tidal, residual, intertidal mudflat (TRIM) model and its applications to San Francisco Bay, California. Estuarine, Coastal and Shelf Science 36, 235–280.

Christiansen, T., Wiberg, P.L., Milligan, T.G., 2000. Flow and sediment transport of a tidal salt marsh surface. Estuarine, Coastal and Shelf Science 50, 315–331.

Cornelissen, G., Gustafsson, O., 2005. Importance of unburned coal carbon, black carbon, and amorphous organic carbon to phenanthrene sorption in sediments. Environmental Science and Technology 39, 764–769.

Cornelissen, G., et al., 2005a. Extensive sorption of organic compounds to black carbon, coal, and kerogen in sediments and solid: mechanisms and consequences for distribution, bioaccumulation, and biodegradation. Environmental Science and Technology 39 (18), 6881–6895.

Cornelissen, G., Haftka, J., Parsons, J., Gustafsson, O., 2005b. Sorption to black carbon of organic compounds with varying polarity and planarity. Environmental Science and Technology 39, 3688–3694.

Fairey, R., et al., 1998. Assessment of sediment toxicity and chemical concentrations in the San Diego Bay region, California, USA. Environmental Toxicology and Chemistry 17, 1570–1581.

Hawker, D.W., Connell, D.W., 1988. Octanol-water partition coefficients of polychlorinated biphenyl congeners. Environmental Science and Technology 22, 382–387.

James, I.D., 2002. Modeling pollution dispersion, the ecosystem and water quality in coastal waters: a review. Environmental Modeling and Software 17, 363–385.

Karickhoff, S.W., David, S., Trudy, A., 1979. Sorption of hydrophobic pollutants on natural sediments. Water Research 13, 241–248.

Krone, B.R., 1962. Flume studies of the transport of sediment in estuarial shoaling processes. Hydraulic Engineering Laboratory, University of California, Berkeley.

Largier, J.L., 1995. San Diego Bay circulation: a study of the circulation of water in San Diego Bay for the purpose of assessing, monitoring and managing the transport and potential accumulation of pollutants and sediment in San Diego Bay, The California State Water Resources Control Board and the California Regional Water Quality Control Board, San Diego Region, San Diego.

Largier, J.L., Hollibaugh, J.T., Smith, S.V., 1997. Seasonally hypersaline estuarines in Mediterranean-climate regions. Estuarine, Coastal and Shelf Science 45, 789–797.

Lumborg, U., Windelin, A., 2003. Hydrography and cohesive sediment modeling: application to the Romo Dyb tidal area. Journal of Marine Systems 38, 287–303.

Martin, J.L., McCutcheon, S.C., 1999. Hydrodynamics and Transport for Water Quality Modeling. Lewis Publishers. 794 pp.

McCain, B.B., et al., 1992. Chemical contamination and associated fish diseases in San Diego Bay. Environmental Science and Technology 26, 725–733.

McDonald, E.T., Cheng, R.T., 1994. Issues related to modeling the transport of suspended sediments in northern San Francisco Bay, California. In: al, M.L.S.e. (Ed.), 3rd International Conference on Estuarine and Coastal Modeling. ASCE, Oak Brook, Illinois, pp. 1–41.

Noblet, J., 2002. Sediment Chemistry in the Southern California Bight: Results from the 1998 Regional Monitoring Study.

Partheniades, E., 1965. Erosion and deposition of cohesive soils. Journal of the Hydraulics Division (ASCE) 91 (HY1), 105–139.

Peng, J., 2004. Integrated geochemical and hydrodynamic modeling of San Diego Bay, California. Ph.D. Dissertation Thesis, University of Southern California, 214 pp.

San Diego Bay Interagency Water Quality Panel, 1994. San Diego Bay 1992 Annual Report. AB 158. Technical Report. California State Water Resources Control Board, Sacramento, CA, USA.

Schwarzenbach, R.P., Westall, John, 1981. Transport of nonpolar organic compounds from surface water to groundwater: laboratory sorption studies. Environmental Science and Technology 15 (11), 1360–1367.

SDSC, 2004. Environmental Data Repository of the Interagency Water Quality Panel and San Diego Supercomputer Center, Website: http://sdbay.sdsc.edu. Access date: June 2004.

Sheng, Y.P., 1996. Pollutant load reduction models for estuaries. In: Spaulding, M.L.a.R.T.C. (Ed.), 4th International Conference on Estuarine and Coastal Modeling. ASCE.

Sheng, P.Y., Eliason, D.E., Chen, X.-J., 1992. Modeling three-dimensional circulation and sediment transport in lakes and estuaries. In: Spaulding, M.Le.a. (Ed.), 2nd International Conferences on Estuarine and Coastal Modeling. ASCE, pp. 109–115.

Sobek, A., Gustafsson, O., Hajdu, S., Larsson, U., 2004. Particle–water partitioning of PCBs in the photic zone: a 25-month study in the open Baltic Sea. Environmental Science and Technology 38, 1375–1382.

Sternberg, R.W., Berhane, I., Ogston, A.S., 1999. Measurement of size and settling velocity of suspended aggregates on the Northern California continental shelf. Marine Geology 154, 43–53.

Taki, K., 2001. Critical shear stress for cohesive sediment transport. In: A.J.M., McAnally, W.H (Eds.), Coastal and Estuarine Fine Sediment Transport. Elsevier Science B.V., pp. 53–61.

Torfs, H., Jiang, J., Mehta, A.J., 2001. Assessment of the erodibility of fine/coarse sediment mixtures. In: A.J.M., McAnally, W.H (Eds.),

Coastal and Estuarine Fine Sediment Processes. Elsevier Science B.V., pp. 109–123.

Van Rijn, L.C., 1989. Handbook—Sediment Transport by Currents and Waves, H461. Delft Hydraulics, Delft, the Netherlands.

Wang, P.-F., et al., 1998. Modeling tidal hydrodynamics of San Diego Bay, California. Journal of American Water Resources Association 34 (5), 1123–1140.

Zeng, E.Y., Peng, J., Tsukada, D., Ku, T.-L., 2002. In-situ measurements of polychlorinated biphenyls in the waters of San Diego Bay, California. Environmental Science and Technology 36 (23), 4975–4980.

Zeng, E.Y., Yu, C.C., Tran, K., 1999. In situ measurements of chlorinated hydrocarbons in the water column off the Palos Verdes Peninsula, California. Environmental Science and Technology 33, 392–398.